

Collective Bayesian Decision-Making in a Swarm of Miniaturized Robots for Surface Inspection

Thiemen Siemensma¹, Darren Chiu², Sneha Ramshanker³, Radhika Nagpal³,
and Bahar Haghighat¹

¹ University of Groningen, Groningen, The Netherlands
{t.j.j.siemensma,bahar.haghighat}@rug.nl

² University of Southern California, Los Angeles, CA, USA chiudarr@usc.edu

³ Princeton University, Princeton, NJ, USA {sr6848,rn1627}@princeton.edu

Abstract. Robot swarms can effectively serve a variety of sensing and inspection applications. Certain inspection tasks require a binary classification decision. This work presents an experimental setup for a surface inspection task based on vibration sensing and studies a Bayesian two-outcome decision-making algorithm in a swarm of miniaturized wheeled robots. The robots are tasked with individually inspecting and collectively classifying a $1m \times 1m$ tiled surface consisting of vibrating and non-vibrating tiles based on the majority type of tiles. The robots sense vibrations using onboard IMUs and perform collision avoidance using a set of IR sensors. We develop a simulation and optimization framework leveraging the Webots robotic simulator and a Particle Swarm Optimization (PSO) method. We consider two existing information sharing strategies and propose a new one that allows the swarm to rapidly reach accurate classification decisions. We first find optimal parameters that allow efficient sampling in simulation and then evaluate our proposed strategy against the two existing ones using 100 randomized simulation and 10 real experiments. We find that our proposed method compels the swarm to make decisions at an accelerated rate, with an improvement of up to 20.52% in mean decision time at only 0.78% loss in accuracy.

1 Introduction

Over the last few decades, automated inspection systems have increasingly become a valuable tool across various industries [8, 24, 25, 7]. Studies have addressed applications in agricultural and hull inspection as well as infrastructure and wind-turbine maintenance [9, 20, 19, 17]. Vibration analysis is a valuable tool in these inspection processes. Different types of vibration analysis are used to detect the condition of infrastructure through structural properties such as modal shapes and eigenfrequencies [2, 21, 12]. A class of inspection tasks involves making a binary decision about a spatially distributed feature of the inspected system. This type of decisions can be effectively addressed by a swarm of robots [30, 26]. When compared to a single entity, swarms improve decision time and accuracy by leveraging collective perception [29, 31]. Moreover, swarms eliminate the problem of sensor-placement and can provide a high-resolution map of

the environment [5, 6]. Collective decision-making algorithms often draw inspiration from nature, such as groups of ants and bees [27]. A more mathematical approach is found in Bayesian algorithms. Applications of Bayesian algorithms have been studied in sensor networks [1, 22] as well as robot swarms [29, 14, 31, 13, 16]. In the study outlined in [13], a collective of agents must determine whether the predominant color of a checkered surface pattern is black or white. The robots function as Bayesian modellers, exchanging information based on two information sharing strategies. The robots either (i) continuously broadcast their ongoing binary observations (*no feedback*) or (ii) continuously broadcast their irreversible decisions once reached (*positive feedback*), pushing the swarm to consensus. A common problem with collective perception methods is slow convergence, i.e. difficulty reaching high belief (probability) about the predominant color. Spatial correlation of observations cause the belief to fluctuate, resulting in long decision times and low decision accuracies, as shown by [14, 4, 3].

In this work, we build on top of the work in [13] in two ways. First, we propose a novel information sharing strategy, named *soft-feedback*. In this approach, binary information is shared between the robots based on their current belief, similar to [28, 4], with the addition of sample variance and random sampling. The resulting strategy is shown to enhance convergence compared to no feedback and positive feedback, without compromising the accuracy of decisions. Second, we move away from the agent-based simulation setup of [13] and present a real experimental setup built around 3-cm-sized vibration sensing wheeled robots. We utilize vibration signals in the presence of measurement noise in place of simulated binary floor color observations. We develop a new sensor board to allow the robots to perform collision avoidance. A digital twin of our experimental setup is developed in Webots, derived from the work done in [10]. We use this model for calibration of our robots and optimization of the algorithm parameters in a Particle Swarm Optimization (PSO) loop.

2 Problem Definition

We task a swarm of N robots to individually inspect and collectively classify a 2D tiled surface section. The surface comprises two types of tiles, vibrating and non-vibrating tiles. The swarm must determine whether the tiled surface is majority vibrating or majority non-vibrating. We denote the fill-ratio f as the proportion of vibrating tiles. Thus, fill-ratios close to 0.5 represent a hard surface inspection problem, as the amount of vibrating and non-vibrating tiles is almost equal. The robots each individually inspect the surface, share their information with the rest of the swarm, and collectively classify the surface. The inspection task ends when every robot in the swarm reaches a final decision, determining if the fill-ratio is above or below 0.5. An underlying real-world scenario could involve inspecting a surface section and determining whether the surface is in a majority *healthy* or in a majority *unhealthy* state.

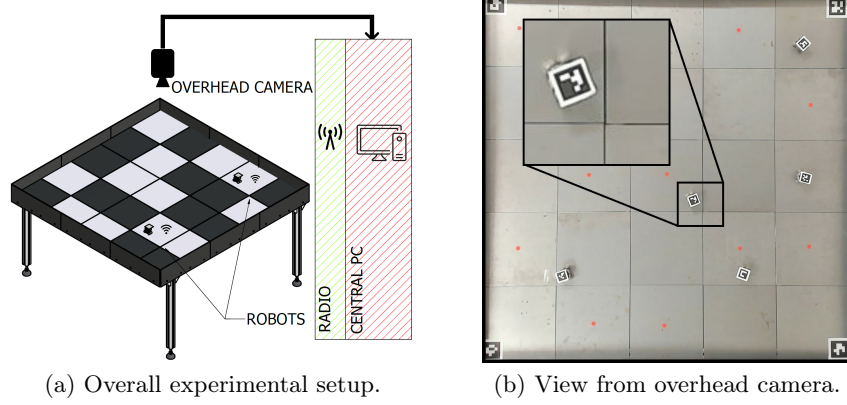


Fig. 1. The experimental setup with a fill ratio of $f = \frac{12}{25} = 0.48$. (a) Schematic overview of the setup is shown. The central PC uses the radio and camera data for analysis. Vibration-motors are attached on the bottom side of white tiles. (b) A snapshot from the overhead camera with detailed view (black square). The red dot markings indicate vibrating tiles. Each robot carries a unique Aruco marker for tracking. Aruco markers in the corners of the environment mark the boundaries.

3 Inspection Algorithm

Algorithm 1 shows our collective Bayesian decision making algorithm. The robots individually estimate and classify the fill ratio f as above or below 0.5. Each robot acts as a Bayesian modeler integrating personal observations and information broadcast by other robots. We consider three information sharing strategies: the (i) no feedback (u^-) and (ii) positive feedback (u^+) strategies, previously studied in [13], and the (iii) soft feedback (u^s) strategy, which we propose in this work.

The robots make binary observations of the surface condition as black/white in simulation or vibrating/non-vibrating in the real setup as $O \in \{0, 1\}$:

$$O \sim \text{Bernoulli}(f) \quad (1)$$

The fill ratio $f \in [0, 1]$ is unknown and is modeled by a Beta-distribution:

$$f \sim \text{Beta}(\alpha, \beta) \quad (2)$$

The prior distribution of f is initialized as $\text{Beta}(\alpha_0 = 1, \beta_0 = 1)$. Upon sampling or receiving observations from other robots, the posterior of f is updated as:

$$f \mid O \sim \text{Beta}(\alpha + O, \beta + (1 - O)) \quad (3)$$

The robots perform a Levy-flight type random walk, moving forward for a time drawn from a Cauchy distribution with mean γ_0 and average absolute deviation γ followed by turning a uniform random angle $\phi \sim U(-\pi, \pi)$ in the direction of $\text{sign}(\phi)$ relative to the forward driving direction. The robots perform collision

Algorithm 1 Collective Bayesian Decision Making

Inputs: $u^-, u^+, u^s, T_{end}, \theta_o, \eta, \theta_c, \tau, p_c$
Initialize: $\alpha = 1, \beta = 1, d_f = -1, \text{robot } id, t_s = 0$
while $t < T_{end}$ **do**
 Perform random walk for τ time
 if $t - t_s > \tau$ **then**
 $O \leftarrow \text{Observation}$ ▷ Get binary observation
 $t_s \leftarrow t$ ▷ Observation timestamp
 $\text{Beta}(\alpha, \beta) \leftarrow \text{Beta}(\alpha + O, \beta + (1 - O))$ ▷ Update modeling of f
 $p \leftarrow P(\text{Beta}(\alpha, \beta) < 0.5)$ ▷ Update belief on f
 $O_{count} \leftarrow O_{count} + 1$ ▷ Observation count
 end if
 if (u^s **Or** $d_f == -1$) **And** ($O_{count} > \theta_o$) **then**
 if $p > p_c$ **then**
 $d_f \leftarrow 0$
 else if $(1 - p) > p_c$ **then**
 $d_f \leftarrow 1$
 end if
 end if
 if u^s **then**
 $\Gamma \leftarrow \text{Var}(\text{Beta})$
 $m \leftarrow \text{Bernoulli}((1 - p)e^{-\eta\Gamma}(\frac{1}{2} - p)^2 + O(1 - e^{-\eta\Gamma}(\frac{1}{2} - p)^2))$
 Broadcast(m) ▷ Soft feedback
 else if (u^+ **And** $d_f \neq -1$) **then**
 Broadcast(d_f) ▷ Positive feedback
 else
 Broadcast(O) ▷ No feedback
 end if
 if Message in queue **then**
 $O \leftarrow \text{Message}$ ▷ Receive message from swarm
 $\text{Beta}(\alpha, \beta) \leftarrow \text{Beta}(\alpha + O, \beta + (1 - O))$ ▷ Update modeling of f
 end if
end while

avoidance upon detecting an obstacle within a range of θ_c millimeters, by turning a random angle $\phi \sim U(-\pi, \pi)$ in the direction of $\text{sign}(\phi)$ relative to the forward driving direction.

Every τ milliseconds a robot samples a new observation O . In simulation, O is based on a binary floor color sampling. In experiments, O is calculated using a 500 millisecond vibration signal sample. The DC component of this sample is removed by employing a first-order high-pass filter with cutoff frequency $\omega_n = 40$ Hz. Given a sampling rate of 350 Hz, the filter parameters α_1 , α_2 , and α_3 are configured to values: 0.20, 0.60, and -0.60 respectively. We define the filtered signal at time step i as \hat{a}_i :

$$\hat{a}_i := \alpha_1 \hat{a}_{i-1} + \alpha_2 a_i + \alpha_3 a_{i-1} \quad (4)$$

where a_i is the magnitude of the IMU's raw acceleration data a_x , a_y , and a_z . The Root-Mean-Square (RMS) of \hat{a} returns the energy of the signal as $\hat{E} = \sqrt{\frac{1}{n} \sum_{i=1}^n \hat{a}_i^2}$. Subsequently, the observation O is determined by comparing \hat{E} with a threshold θ_E :

$$O = \begin{cases} 1 & \text{if } \hat{E} > \theta_E \\ 0 & \text{if } \hat{E} \leq \theta_E \end{cases} \quad (5)$$

We consider three information sharing strategies. (i) No feedback (u^-) considers sharing the latest observation O in any case. (ii) Positive feedback (u^+) is similar to (u^-) until reaching a final decision. From this point in time it broadcasts its irreversible final decision d_f . The intuition behind positive feedback is to push the swarm to consensus upon reaching a final decision by one robot. However, this is not very effective when no robot is able to reach a final decision. In this case, positive feedback is not different from no feedback. To resolve this, we propose soft-feedback (iii). Soft feedback (u^s) broadcasts a binary value sampled from a Bernoulli distribution. The corresponding probability is calculated through the soft feedback parameter $\eta \in \mathbb{R}^+$, the current observation $O \in \{0, 1\}$, and the current belief $p \in [0, 1]$ as below:

$$m \sim \text{Bernoulli}(\delta \cdot (1 - p) + (1 - \delta) \cdot O) \quad (6a)$$

$$\delta = e^{-\eta\Gamma} \left(\frac{1}{2} - p\right)^2 \quad (6b)$$

$$p = P(\text{Beta}(\alpha, \beta) < 0.5) \quad (6c)$$

where $m \in \{0, 1\}$ is the outgoing message, Γ is the variance of the Beta distribution and p is the robot's belief evaluated as the CDF of the Beta distribution at $f = 0.5$. The intuition behind soft-feedback is to broadcast information that is initially incorporating only the observation O , but gradually factors in more of the belief p . Namely, Equation 6b depends on (i) a compelling component $e^{-\eta\Gamma} \in [0, 1]$ which increases the proportion of the current belief in messages as Γ decreases, and (ii) a stabilizing component $(\frac{1}{2} - p)^2 \in [0, 0.25]$ which is the squared distance of p from the indecisive state $p = 0.5$, increasing the proportion of robot's belief in the Bernoulli sampled message to enhance accuracy. This prevents the robot from prematurely making a decision with low confidence.

Upon reaching a minimum of θ_o number of observations, a robot considers making a final decision based on its belief p . If above the credibility threshold $p > p_c$, the robot's final decision d_f is set to 1. Conversely, if $(1 - p) > p_c$, d_f is set to 0. The inspection task ends when all robots have made a final decision.

4 Real Experimental Setup

Our experimental setup, shown in Figure 1, is built around (i) a tiled surface section of size $1\text{m} \times 1\text{m}$, and (ii) a swarm of 3cm-sized vibration-sensing wheeled robots that traverse and inspect the tiled surface section. The surface section consists of 25 tiles, each of size $20\text{cm} \times 20\text{cm}$, that are laid out in a square grid with

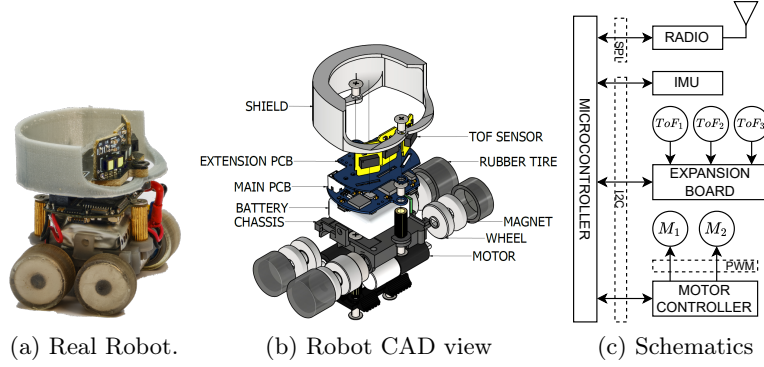


Fig. 2. We use a revised and extended version of the original Rovable robot [9]. (a) The extended robot with IR sensor board. (b) Exploded 3D CAD view of the extended robot. (c) Electronic block diagram of the extended robot. The microcontroller (Atmel SAMD21G18) interfaces with the IMU (MPU6050), 2.4 GHz radio (nRF24L01+), motor-controllers (DRV8835), and ToF IR sensors (VL53L1X).

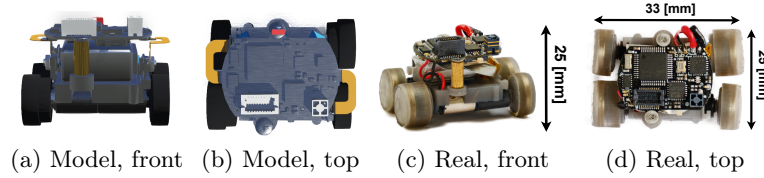


Fig. 3. We use a simpler robot model in simulation, with IR sensors directly simulated on the main PCB. Our simulated collision avoidance closely matches reality.

five tiles on each side. There are two types of tiles on the surface, vibrating and non-vibrating tiles. The vibrating tiles are excited using two miniature vibration motors mounted on top of one another underneath the tile at its center (ERM 3V Seed Technology motors). All tiles are secured to an aluminium frame using 2cm \times 1cm pieces of magnetic tape around the corners. The frame consists of four strut profiles in the middle and four others along the edges of the arena. We use an overhead camera (Logitech BRIO 4k) and Aruco markers for visual tracking of the robots.

We use a revised and extended version of the Rovable robot originally presented in [11]. As shown in Figure 2, each robot measures 25mm \times 33mm \times 35mm and carries two customized Printed Circuit Boards (PCBs): (i) a main PCB hosting the microcontroller, an IMU, motor controllers, power circuitry and radio and (ii) an extension PCB hosting IR sensors for collision avoidance. The main PCB has essentially the same design as the one in [11], and was only revised and remade for updated components. The extension PCB is new and hosts three small Time-of-Flight (ToF) IR sensor boards, each facing a direction of 0°, 25°, and -25° relative to the forward driving direction of the robot. Each sensor has a field of view of 27° and a range of up to 1m. A 3D printed shield is mounted around the extension PCB to enhance the visibility of the robot when perceived by the IR sensors of other robots. The robot has four magnetic wheels. Only two wheels, one on the front and one on the back, are driven by PWM operated motors. At 100% PWM, the robot drives forward at around 5cm per second.

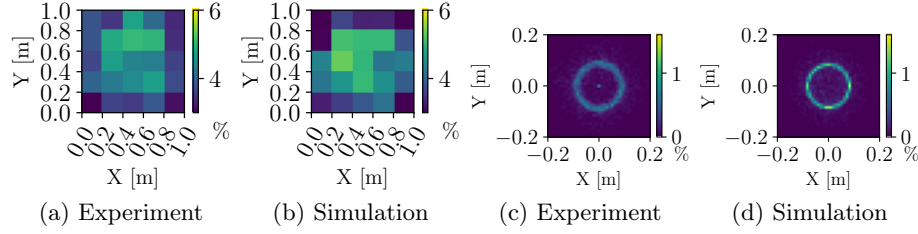


Fig. 4. Distribution of samples across tiles in real (a) and simulated (b) setups. The displacement between consecutive samples in real (c) and simulated (d) setups.

5 Simulation and Optimization Framework

Our simulation framework provides a virtual environment where we can study the operation of our robot swarm. Within Webots, we set up two main components: (i) a realistic model of our robot, and (ii) a tiled surface that the robots inspect, with a black and white projected floor pattern. We use the black and white tiles in simulation as a proxy for vibrating and non-vibrating tiles in our real experimental setup. In simulation, we assume noise-free binary sampling of the surface and zero loss on inter-robot communication. Figure 3 shows the simulated and the real robots side by side. In simulation, the ToF sensor board is absent, but simulated IR sensors retain comparable range and positioning. We recreate mechanical differences that exist between real robots by adding randomized offsets to the simulated left and right motor speed commands:

$$M_l^s \leftarrow M_l^s r_v (1 - r_a) \quad (7a)$$

$$M_r^s \leftarrow M_r^s r_v (1 + r_a) \quad (7b)$$

where M_l^s and M_r^s are the left and right motor speeds, and r_v and r_a are drawn from empirically chosen uniform distributions $U \sim (0.95, 1.05)$ and $U \sim (-0.125, 0.125)$, respectively. We calibrate our simulation empirically considering three characteristic features: (i) sample distribution over the experimental setup, (ii) time between consecutive samples, and (iii) distance between consecutive samples. To obtain data for our calibrations, we run experiments using five robots for 3×20 minutes with algorithm parameters $[\gamma, \gamma_0, \tau, \theta_c] = [5000, 2000, 1500, 60]$ using the u^- information sharing strategy (Section 3). The Pearson correlation coefficients for the obtained data (partly shown in Figure 4) corresponding to the three features mentioned above are calculated as 0.990, 0.984, and 0.735, respectively. These values confirm the similarity between simulated and real swarm behaviors, enabling optimizing real experiments using simulation.

Our optimization framework involves two components: (i) our calibrated simulation and (ii) a noise-resistant PSO method. Throughout the PSO iterations, every particle is evaluated multiple times on randomized floor patterns with the same fill-ratio. The velocity and position of particle i are updated at iteration k as:

$$\mathbf{v}_i^{k+1} = \omega \cdot \mathbf{v}_i^k + \omega_p \cdot \mathbf{r}_1 (\mathbf{p}_{b_i} - \mathbf{p}_i^k) + \omega_g \cdot \mathbf{r}_2 (\mathbf{g}_b - \mathbf{p}_i^k) \quad (8a)$$

$$\mathbf{p}_i^{k+1} = \mathbf{p}_i^k + \mathbf{v}_i^{k+1} \quad (8b)$$

where \mathbf{v}_i^k and \mathbf{p}_i^k are the velocity and position vector of particle i at iteration k . \mathbf{p}_{b_i} and \mathbf{g}_b correspond to the position vector of the personal best and global best evaluations for particle i , respectively. We set the PSO weights for inertia, personal best, and global

best as $[\omega \ \omega_p \ \omega_g] = [0.75 \ 1.5 \ 1.5]$, balancing local and global exploration [23, 15, 18]. The values \mathbf{r}_1 and \mathbf{r}_2 are drawn from a uniform distribution $U \sim (0, 1)$ each iteration.

6 Experiments and Results

We use a swarm of five robots, all employing $p_c = 0.95$, and floor patterns with a fill ratio of $f = 0.48$ to conduct simulation and real experiments. We evaluate on decision time and accuracy for the strategies u^- , u^+ , and u^s . We consider decision time as the time the last robot that makes a final decision. We average the beliefs (Equation 6c) of the robots at this decision time to calculate a corresponding decision accuracy. We do not incorporate any base-line method, as this was already shown in [13].

6.1 Simulation Experiments

Five algorithmic parameters determine the sampling behavior of the swarm. These include mean (γ_0) and mean absolute deviation (γ) of the Cauchy distribution characterizing the robots' random walk, the sampling interval (τ), the collision avoidance threshold (θ_c), and the observations threshold (θ_o). Table 1 lists the boundaries of our optimization search space. The lower bounds for τ and θ_c are set to allow smooth pause-sample-move and collision avoidance maneuvers. The bounds on γ and γ_0 are set such that a robot is able to cross the arena in one random walk step. The bounds on the observation threshold θ_o are established empirically. The particles in the PSO swarm are initialized randomly within the bounded search space, with the exception of one particle P_0 set to an empirically chosen location. Each particle is evaluated multiple times to mitigate randomness. For a particle i , we define the performance cost \mathcal{C}_i as:

$$\mathcal{C}_i = \mu \left([c_1 \ c_2 \ \dots \ c_{N_e}]^\top \right) + 1.1 \cdot \sigma \left([c_1 \ c_2 \ \dots \ c_{N_e}]^\top \right) \quad (9)$$

where N_e is the number of re-evaluations and c_j is the outcome of the evaluation j :

$$\epsilon_i(t, d_f) = \begin{cases} \epsilon_f \cdot t / T_{end} & d_f = d_f^* \\ \epsilon_f \cdot \epsilon_d & d_f \neq d_f^* \\ \epsilon_f & d_f = -1 \end{cases} \quad (10a)$$

$$c_j = \sum_{i=1}^{N_r} \epsilon_i \quad (10b)$$

where $N_r = 5$ is the number of robots, ϵ_i is the performance cost of robot i for which the robot's final decision d_f made at time t is compared with the correct decision

Table 1. The PSO optimization parameters and bounds. P_0 is the empirical best guess particle. P^* is the resulting best particle with respect to our cost-function.

Parameter	γ_0 [ms]	γ [ms]	τ [ms]	θ_c [mm]	θ_o
P_0	2000	5000	2000	60	50
\min_i	2000	0	1000	50	50
\max_i	15000	15000	3000	100	200
P^*	7565	15000	2025	50	85

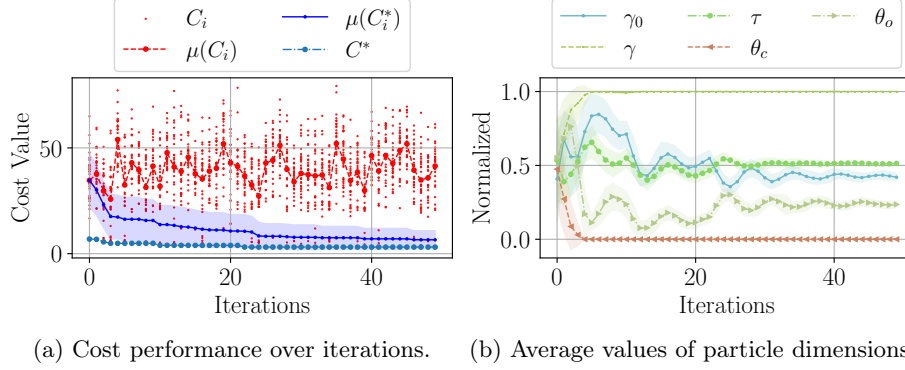


Fig. 5. We use 30 particles, each re-evaluated 16 times, over 50 iterations using Equation 9. (a) Progression of cost performance of each particle (C_i), personal best cost performance of each particle (C_i^*), and the global best cost performance (C^*). (b) Progression of mean and standard deviation of parameters in Table 1.

d_f^* . A wrong decision is penalized by a factor of $\epsilon_d = 5$. The value $\epsilon_f = 1 + |f - f^*|/\epsilon_t$ is calculated using the absolute difference between a robot's current estimate of the fill ratio $f = \alpha/(\alpha + \beta)$ and the correct fill ratio f^* , divided by a normalizing factor $\epsilon_t = 0.04$ that corresponds to the contribution of one tile in the overall 25-tile setup.

To find the optimal parameters for our inspection algorithm, we first consider running the algorithm with the u^- information sharing strategy through our optimization framework. Our intuition is that an optimal parameter set for u^- should allow the swarm to obtain a well-representative sample of the environment in a time-efficient manner, thus, the same parameters should also perform optimally for u^+ and u^s . Using this parameter set, we then run a systematic search to find an optimal value for the soft feedback parameter η that characterizes the u^s information sharing strategy.

We consider the u^- strategy first. For the PSO optimizations, we use 30 particles, 50 iterations, and 16 re-evaluations. Each particle is evaluated for $T_{end} = 1200s$ or until all robots in the swarm have reached a decision. The optimization results are shown in Figure 5. It can be seen that the average personal best performance of the particles converges to the performance of the global best particle P^* , which is listed in Table 1.

Using P^* , we then run a systematic search for the soft-feedback parameter η . We consider five candidate values for η based on prior empirical tests and run 100 randomized simulations to evaluate the performance of u^s against u^- and u^+ . Figure 6 illustrates the results. We see that u^s consistently outperforms u^- and u^+ in decision time. Regarding accuracy, u^s closely approaches the performance of u^+ and u^- at $\eta = 1000$. Specifically, for $\eta = 1000$, the u^s achieves a 20.52% reduction in mean decision time at a 0.78% loss in accuracy, compared with u^+ . When compared with u^- , u^s achieves a reduction of 22.10% in mean decision time at a 1.22% loss in accuracy.

To assess the generalizability of our findings, we run 100 randomized simulations across fill-ratios of $f \in [0.44, 0.48, 0.52, 0.56]$ to compare u^- , u^+ and u^s (with $\eta = 1000$) based on decision time and accuracy. Each simulation ends upon reaching T_{end} or when all robots have reached a decision. For a fair comparison, we fix the random seeds used to generate floor patterns across the simulation instances. Figure 6c shows that u^s outperforms the other two strategies in decision time. Due to incorporating beliefs

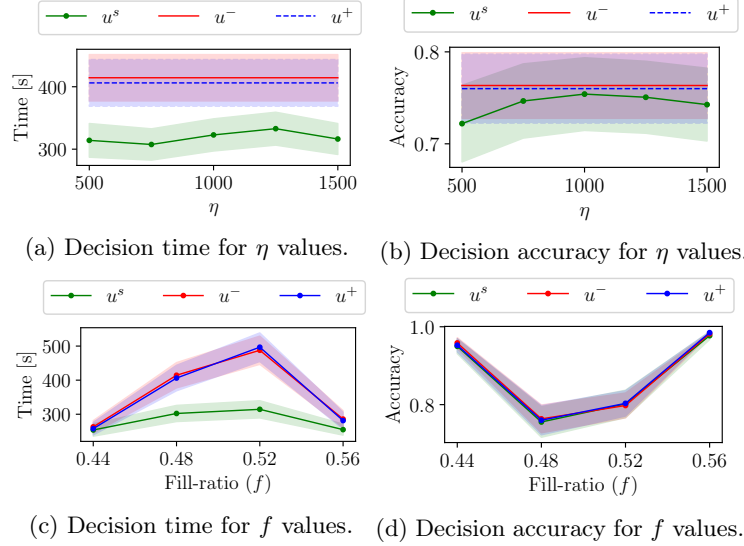


Fig. 6. Decision time (a) and decision accuracy values (b) of 100 randomized simulation experiments using systematic search for the soft-feedback parameter η of u^s , compared against u^- and u^+ . Using $\eta = 1000$ we run 100 randomized simulations for different $f \in [0.44, 0.48, 0.52, 0.56]$ and compare with u^- and u^+ . The resulting decision times and accuracies are shown in (c) and (d), respectively.

in messages, the swarm is compelled to make a decision rapidly, reducing mean and variation in decision times. This is particularly beneficial in harder environments where the fill ratio is close to $f = 0.5$, facilitating reaching the credibility threshold p_c .

6.2 Real Experiments

We validate our simulation results by real experiments in 10 trials for u^- , u^+ , and u^s . We first tune the sample threshold θ_E using data from one hour of swarm operation employing u^- and algorithm parameters $[\gamma, \gamma_0, \tau, \theta_c] = [5000, 2000, 1000, 60]$, gathering a total of 6975 samples. Our evaluation criteria are the number of false observations and the fill-ratio error $|f - f^*|$. Figure 7 shows that we obtain $|f - f^*| \approx 0$ at $\theta_E = 1.55$. Employing $\theta_E = 1.55$ results in an equal amount of False Positives (FP) and False Negatives (FN), balancing the modeling error on the Beta distribution. Furthermore, we note that false observations appear mostly along edges of the tiles. This is expected as robots may sample close to the tile edges while they are in contact with two tiles.

We conduct 10 experimental trials on our experimental setup with $f^* = 0.48$ for assessing u^- , u^+ and u^s . The real experiments confirm our findings in simulation and reveal that the utilization of u^s notably decreases the swarm’s decision time. Employing u^s compels the swarm to reach decisions at an accelerated rate compared to u^+ and u^- . The decision time and accuracy data from real experiments is shown in Figure 8. We can see that u^s demonstrates inherently less variance in decision times. Moreover, we encounter fewer indecisive trial outcomes with u^s compared to u^+ and u^- .

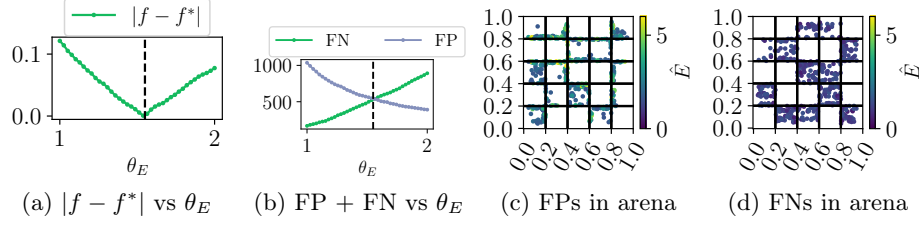


Fig. 7. The threshold parameter θ_E determines binary observations of vibration data in real experiments (see Equation 5). (a) The fill ratio error $|f - f^*|$ for different values of θ_E (0.025 grid). (b) False observations for different values of θ_E (c) Spatial distribution of false positive and (d) false negative observations.

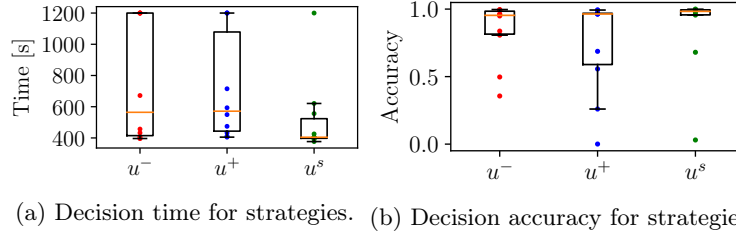


Fig. 8. Decision time and accuracy in real experiments with a fill-ratio of $f = 0.48$ for different information sharing strategies. If no decision is made within $t = T_{end}$, we refer to $T_{end} = 1200s$ for decision time and the corresponding belief at the end of the simulation experiment for accuracy. We see that u^s is faster and equally accurate as u^- and u^+ in real experiments, confirming our findings in simulation experiments.

7 Conclusion and Future Work

In this work, we presented an experimental setup for studying a surface inspection task using a swarm of vibration sensing robots and explored the application of a Bayesian decision-making algorithm. We developed a simulation framework leveraging the physics based Webots robotic simulator and a PSO method to optimize the parameters shaping the robots' sampling performance. The resulting optimal parameter values were assessed for three information sharing strategies in randomized simulations across different environments based on the swarm's decision time and accuracy. We observed that our proposed soft feedback strategy yields a significant decrease in decision time without a major compromise in decision accuracy, compared to two previously studied strategies. Furthermore, hardware experimental trials validated our simulation findings. In real experiments, no drop in the decision accuracy was observed, demonstrating the adaptability and robustness of the decision-making processes to noise. In our future work, we plan to increase the complexity of our experiments in several ways, considering (i) performing inspection of complex structures such as 3D surfaces or obstacle-dense environments, (ii) classifying time-varying fill-ratios on our experimental setup, and (iii) studying the effect of the swarm size on the inspection performance.

References

1. Alanyali, M., Venkatesh, S., Savas, O., Aeron, S.: Distributed bayesian hypothesis testing in sensor networks. In: Proceedings of the American Control Conference. vol. 6, pp. 5369–5374. Institute of Electrical and Electronics Engineers Inc. (2004). <https://doi.org/10.23919/acc.2004.1384706>
2. Arnaud Deraemaeker, Keith Worden: New Trends in Vibration Based Structural Health Monitoring. Springer Vienna (2010)
3. Bartashevich, P., Mostaghim, S.: Benchmarking collective perception: New task difficulty metrics for collective decision-making. In: Lecture Notes in Computer Science (including subseries Lecture Notes in Artificial Intelligence and Lecture Notes in Bioinformatics). vol. 11804 LNAI, pp. 699–711. Springer Verlag (2019). https://doi.org/10.1007/978-3-030-30241-2{_}58
4. Bartashevich, P., Mostaghim, S.: Multi-featured collective perception with Evidence Theory: tackling spatial correlations. *Swarm Intelligence* **15**(1-2), 83–110 (2021). <https://doi.org/10.1007/s11721-021-00192-8>
5. Bayat, B., Crasta, N., Crespi, A., Pascoal, A.M., Ijspeert, A.: Environmental monitoring using autonomous vehicles: a survey of recent searching techniques (2017). <https://doi.org/10.1016/j.copbio.2017.01.009>
6. Bigoni, C., Zhang, Z., Hesthaven, J.S.: Systematic sensor placement for structural anomaly detection in the absence of damaged states. *Computer Methods in Applied Mechanics and Engineering* **371** (2020). <https://doi.org/10.1016/j.cma.2020.113315>
7. Bousdekis, A., Apostolou, D., Mentzas, G.: Predictive Maintenance in the 4th Industrial Revolution: Benefits, Business Opportunities, and Managerial Implications. *IEEE Engineering Management Review* **48**(1), 57–62 (2020). <https://doi.org/10.1109/EMR.2019.2958037>
8. Brem, C., Siemens: Senseye Predictive Maintenance - Whitepaper True Cost Of Downtime 2022 (2023)
9. Carbone, C., Garibaldi, O., Kurt, Z.: Swarm Robotics as a Solution to Crops Inspection for Precision Agriculture. *KnE Engineering* **3**(1), 552 (2018). <https://doi.org/10.18502/keg.v3i1.1459>
10. Chiu, D., Nagpal, R., Haghighat, B.: Optimization and Evaluation of Multi Robot Surface Inspection Through Particle Swarm Optimization. In: ICRA. pp. 8996–9002 (2024)
11. Dementyev, A., Kao, H.L.C., Choi, I., Ajilo, D., Xu, M., Paradiso, J.A., Schmandt, C., Follmer, S.: Rovables: Miniature on-body robots as mobile wearables. In: UIST 2016 - Proceedings of the 29th Annual Symposium on User Interface Software and Technology. pp. 111–120. Association for Computing Machinery, Inc (2016). <https://doi.org/10.1145/2984511.2984531>
12. Doebling, S., Farrar, C., Prime, M., Shevitz, D.: Damage identification and health monitoring of structural and mechanical systems from changes in their vibration characteristics: A literature review. Tech. rep. (1996)
13. Ebert, J.T., Gauci, M., Mallmann-Trenn, F., Nagpal, R.: Bayes Bots: Collective Bayesian Decision-Making in Decentralized Robot Swarms. In: ICRA (2020). <https://doi.org/10.1109/ICRA40945.2020.9196584>
14. Ebert, J.T., Gauci, M., Nagpal, R.: Multi-Feature Collective Decision Making in Robot Swarms. In: Proc. of the 17th International Conference on Autonomous Agents and Multiagent Systems (AAMAS). vol. 9 (2018)

15. Gad, A.G.: Particle Swarm Optimization Algorithm and Its Applications: A Systematic Review. *Archives of Computational Methods in Engineering* **29**(5), 2531–2561 (2022). <https://doi.org/10.1007/s11831-021-09694-4>
16. Haghighat, B., Ebert, J., Boghaert, J., Ekblaw, A., Nagpal, R.: A Swarm Robotic Approach to Inspection of 2.5 D Surfaces in Orbit (2022)
17. Halder, S., Afsari, K.: Robots in Inspection and Monitoring of Buildings and Infrastructure: A Systematic Review (2023). <https://doi.org/10.3390/app13042304>
18. Innocente, M.S., Sienz, J.: Coefficients’ Settings in Particle Swarm Optimization: Insight and Guidelines. *Mecánica Computacional: Computational Intelligence Techniques for Optimization and Data Modeling* **XXIX**, 9253–9269 (2010)
19. Lee, A.J., Song, W., Yu, B., Choi, D., Tirtawardhana, C., Myung, H.: Survey of robotics technologies for civil infrastructure inspection. *Journal of Infrastructure Intelligence and Resilience* **2**(1), 100018 (2023). <https://doi.org/10.1016/j.iintel.2022.100018>
20. Liu, Y., Hajj, M., Bao, Y.: Review of robot-based damage assessment for offshore wind turbines (2022). <https://doi.org/10.1016/j.rser.2022.112187>
21. Magalhães, F., Cunha, A., Caetano, E.: Vibration based structural health monitoring of an arch bridge: From automated OMA to damage detection. *Mechanical Systems and Signal Processing* **28**, 212–228 (2012). <https://doi.org/10.1016/j.ymssp.2011.06.011>
22. Makarenko, A., Durrant-Whyte, H.: Decentralized Bayesian algorithms for active sensor networks. *Information Fusion* **7**(4 SPEC. ISS.), 418–433 (2006). <https://doi.org/10.1016/j.inffus.2005.09.010>
23. Poli, R., Kennedy, J., Blackwell, T.: Particle swarm optimization. *Swarm Intelligence* **1**(1), 33–57 (2007). <https://doi.org/10.1007/s11721-007-0002-0>
24. PwC: PdM 4.0. Tech. rep. (2017)
25. Roda, I., Macchi, M., Fumagalli, L.: The future of maintenance within industry 4.0: An empirical research in manufacturing. In: *IFIP Advances in Information and Communication Technology*. vol. 536, pp. 39–46. Springer New York LLC (2018). https://doi.org/10.1007/978-3-319-99707-0_{_}6
26. Schranz, M., Umlauf, M., Sendel, M., Elmenreich, W.: Swarm Robotic Behaviors and Current Applications (2020). <https://doi.org/10.3389/frobt.2020.00036>
27. Seeley, T.D., Buhrman, S.C.: Group decision making in swarms of honey bees. *Behav Ecol Sociobiol* **45**, 19–31 (1999)
28. Shan, Q., Mostaghim, S.: Discrete collective estimation in swarm robotics with distributed Bayesian belief sharing. *Swarm Intelligence* **15**(4), 377–402 (2021). <https://doi.org/10.1007/s11721-021-00201-w>
29. Valentini, G., Brambilla, D., Hamann, H., Dorigo, M.: Collective Perception of Environmental Features in a Robot Swarm **9882** (2016). <https://doi.org/10.1007/978-3-319-44427-7>
30. Valentini, G., Ferrante, E., Dorigo, M.: The best-of-n problem in robot swarms: Formalization, state of the art, and novel perspectives (2017). <https://doi.org/10.3389/frobt.2017.00009>
31. Valentini, G., Ferrante, E., Hamann, H., Dorigo, M.: Collective decision with 100 Kilobots: speed versus accuracy in binary discrimination problems Collective decision with 100 Kilo-bots: speed versus accuracy in binary discrimination problems. *Autonomous Agents and Multi-Agent Systems* **30**(3), 553–580 (2016). <https://doi.org/10.1007/s10458-015-9323-3>